Shock waves propagating in a channel with obstacles

Francesco S. Marra[1] **and Marcello Manna**[2]

(1) Istituto di Ricerche sulla Combustione - CNR
Via Diocleziano 328, Napoli Italy (marra@irc.na.cnr.it)
(2) Dipartimento di Ingegneria Meccanica per l'Energetica
Università "Federico II", Via Claudio 21, Napoli Italy (manna@unina.it)

Abstract

A numerical study of the dissipation effects due to the presence of repeated obstacles on the strength of propagating shock waves in a channel is performed. The compressible Navier-Stokes equations are numerically solved, taking into account for the dissipation effects. The influence of varying the Mach number and the spacing of the obstacles on the attenuation of the shock strength is investigated. A preliminar attempt is made to measure how the energy scattering is affected by the different size of obstacles and shock strengths, in order to identify the leading energy transfer mechanisms affecting the formation of hot spots.

Introduction

Up today it is not fully understood how many mechanisms are involved in the propagation of a deflagration and in its transition to detonation, but it clearly appears, both from experimental and numerical analysis, that the onset of a detonation is likely to be initiated by the presence of hot spots behind a shock wave [1]. This kind of small regions can occur in various circumstances; amongst many other shock turbulence interaction, shock boundary layer interaction, and shock flame interaction, must be mentioned. In all cases quantitative results concerning the occurrence of a sufficiently strong hot spot for the detonation to be initiated are not close in hands.

In this study we focus on the more simple configuration of a shock wave propagating in an inert confined mixture (air), with the eventual aim of determining which are the leading energy transfer mechanisms affecting the formation of hot spots. One of the key point to address is the fact that, in the case of a planar shock wave, the presence of the confinement causes a scattering of the energy in all possible components, and this augments the amount of energy that is dissipated, diminishing the strength of the shock itself.

Herein a preliminar attempt is made to measure how the energy scattering is affected by the different size of obstacles and shock strengths. To this aim highly resolved numerical solution of the compressible Navier-Stokes equations have been carried out. This level of simulation is believed to be mandatory if physical dissipative mechanisms have to be accounted for.

Governing Equations

The flow fields we are concerned with are governed by the (2D, i.e. $i = 1, 2$) compressible Navier-Stokes equations which read:

$$\frac{\partial}{\partial t}\rho + \frac{\partial}{\partial x_j}\left(\rho u_j\right) \tag{1}$$

$$\frac{\partial}{\partial t}\left(\rho u_i\right) + \frac{\partial}{\partial x_j}\left(\rho u_i u_j + p\delta_{ij}\right) = \frac{\partial}{\partial x_j}\left(\tau_{ij}\right) \tag{2}$$

$$\frac{\partial}{\partial t}\left(\rho e_t\right) + \frac{\partial}{\partial x_j}\left(\left(\rho e_t + p\right) u_j\right) = \frac{\partial}{\partial x_j}\left(\tau_{ij} u_i\right) + \frac{\partial}{\partial x_j}\left(\kappa \frac{\partial}{\partial x_j} T\right) \tag{3}$$

$$\tau_{ij} = 2\mu\left(S_{ij} - \frac{1}{3}\frac{\partial u_k}{\partial x_k}\delta_{ij}\right) \qquad S_{ij} = \frac{1}{2}\left(\frac{\partial u_i}{\partial x_j} + \frac{\partial u_j}{\partial x_i}\right)$$

where standard tensor notation has been employed. In the previous relations the quantities ρ, u_i, e_t, p, T are the density, the velocity components, the total energy per unit mass, the pressure, and the absolute temperature, respectively. The gas is assumed to be calorically perfect. The thermal conductivity κ is evaluated from the Prandtl number and the specific heat at constant pressure $\kappa = c_p\mu/Pr$, where the molecular viscosity μ is related to the temperature according to Sutherland's law.

Following the classical finite volume formulation the integral form of eq. (1,2,3) is discretized on a set of non overlapping quadrangular elements. The flow solver enjoys the flexibility of a patching domain decomposition technique with conformal interfaces. The convective terms are evaluated by means of Roe's approximated Riemann solver whose interface values are obtained trough a quadratic reconstruction procedure according to the MUSCL approach. The limiter function is applied to the characteristic variables. The diffusive terms are centrally discretized on a dual grid. Time advancement is carried out through a TVD 3 stage Runge-Kutta method [2]. The time step computation is based on positivity condition for the non linear scalar convection equation whose speed is given by the largest eigenvalue of the Euler system. Viscous time step restrictions are also accounted for. Additional details concerning the flow solver can be found in [3].

Results

The configuration investigated herein, consists of a channel roughned with eight obstacles of height h so that the relevant non dimensional geometrical parameter is $R = H/h$ (see fig. 1). The initial conditions

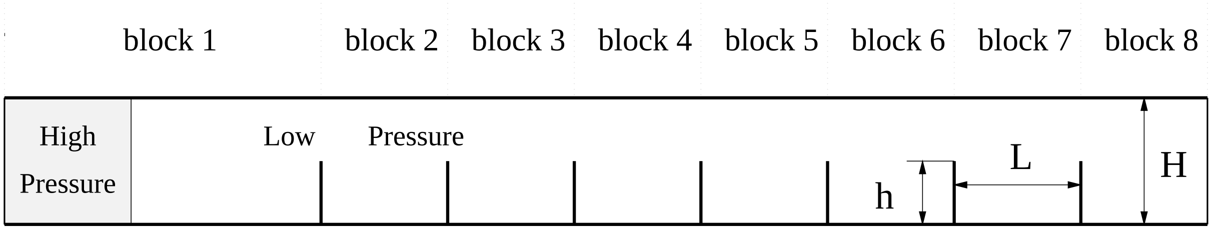

Figure 1: Channel Geometry

are determined as two constant states separated by a membrane which is ruptured at $t = 0$. The states are such that the solution to the corresponding one-dimensional Riemann problem (in absence of obstacles) generates a shock wave of prescribed strength. Two strengths have been investigated, i.e. $M_s = v_s/\sqrt{\gamma p/\rho} = 1.4, 2.0$ and $Re = v_s H/\nu = 5000$, where M_s is the shock wave Mach number and Re is the Reynolds number. Actually M_s was varied in a larger range, but only two cases are presented below, for the sake of brevity. The Reynolds number was selected small enough that grid converged solutions, in the sense of local truncation error, could be achieved. Following a mesh refinement study the final grid configuration consisted of seven blocks of 121×121 points plus a front block of 161×121 points. The simulations are direct, in the sense that neither time averaging, nor space averaging of the governing equations is carried out. Thus no turbulence closure is employed. Because the principal mechanism for energy re-distribution between large and small turbulence scales is inhibited by the two dimensional character of the computations, the results presented herein have to be considered with caution. However, since the leading dissipation mechanism for these class of problems is believed to be associated with the interaction of the blast wave with the obstacles we conjecture that a fully three dimensional simulation will not substantially change the conclusions attained in this study. Currently we are undertaking the effort of a 3D computation to assert the above claims.

In fig. 2 we present the computed locations of the shock wave front versus time against the theoretical values obtained from the Riemann problem solution. The values of x_s are representative of an equivalent one dimensional field which is extracted out of the two dimensional instantaneous data set through a transverse section area averaging procedure. Since the leading shock front is curved, as a results of the interaction with the obstacles, the definition of x_s is somewhat arbitrary. We define x_s as the rightmost location where the relative change of static pressure exceeds by 1% the undisturbed flow field value. We can clearly see that, irrespectively of the M_s value, the presence of the obstacles slows down the blast wave considerably (for $R = 2$ as much as 17%). In addition the strength of the shock is largely reduced. From a safety point of view one important issue is a correct estimate of the shock attenuation. To this aim we have reported in fig. 3 the maximum instantaneous pressure locally reached over the whole 2D channel versus the non dimensional time $\tau = t/t_f$ where t_f is the ending time of each simulation, which corresponds to the overtaking of the last obstacle. The pressure values have been normalized with their corresponding reservoir conditions. We observe that the higher the Mach number the stronger the relative maximum pressure reduction. Actually the trend is a non monotone decreasing function of

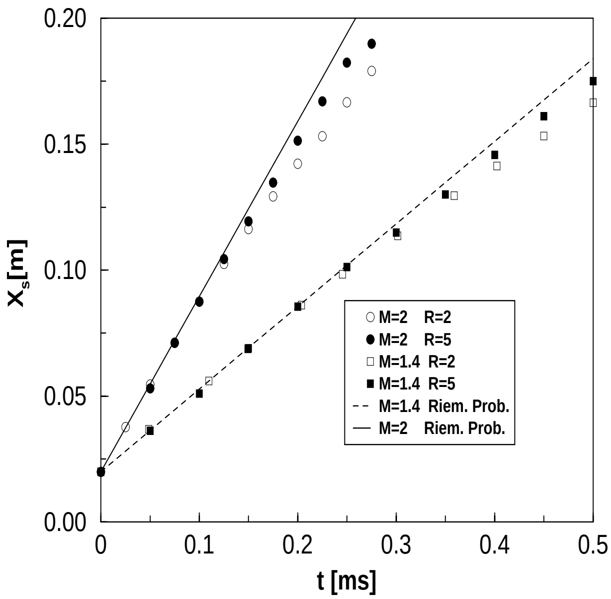

Figure 2: Shock Location versus Time

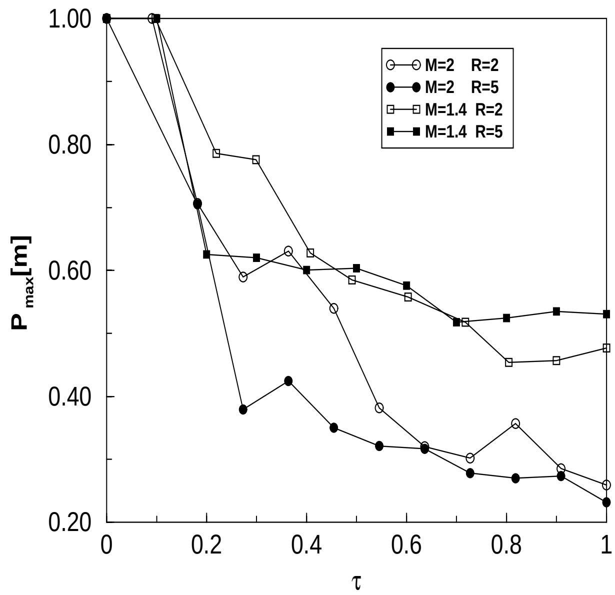

Figure 3: Maximum Pressure versus Time

time. The local maximum pressure rise at $\tau \approx 0.38$ ($M_s = 2.0 \;\; R = 2$) is determined by the incident shock interactions with the first obstacle. In figure 4 we present a few Mach number shaded plots for both $M_s = 2$ (upper set) and $M_s = 1.4$ (lower set). Inspecting the shock strengths at the channel exit we concluded that a very strong attenuation (measured as the ratio of the final over the initial Mach jump) is taking place. The above mentioned ratios heavly depend upon the value of M_s; in particular $\Delta M(\tau = 1)/\Delta M(\tau = 0)$ ranges from 0.12 for the $M_s = 1.4$ to 0.56 for the $M_s = 2$ case ($R = 2$). Also, the complicated flow patterns taking place in the channel (see for instance the large shock-wave boundary layer interaction at $x \approx 0.03$ for the $M_s = 2$ case), cannot be accounted for in a one dimensional quasi 1D flow computation with a friction law. Let us assume that the latter is calibrated to best fit the present data; to be on the safe side we should then tune the friction law in such a way that the local maximum is predicted. By doing so we would largely overestimate the shock strength at the end of the interaction.

References

[1] H. Kleine, R. Knystautas and J. H. S.. Lee, The Effect of Turbulence on Reflected Shock Ignition and the Initiation of Detonation, 16th ICDERS Proceedings, Cracow, August 1997.

[2] C. Shu, High Order ENO and WENO Schemes for Computational Fluid Dynamics, in Higher Order Discretization Methods in Computational Fluid Dynamics, RTO-AVT/VKI Special Course, September 1998.

[3] M. Manna, A Three Dimensional High Resolution Compressible Flow Solver, PhD Thesis, Catholic University of Louvain/von Karman Institute for Fluid Dynamics, 1992.

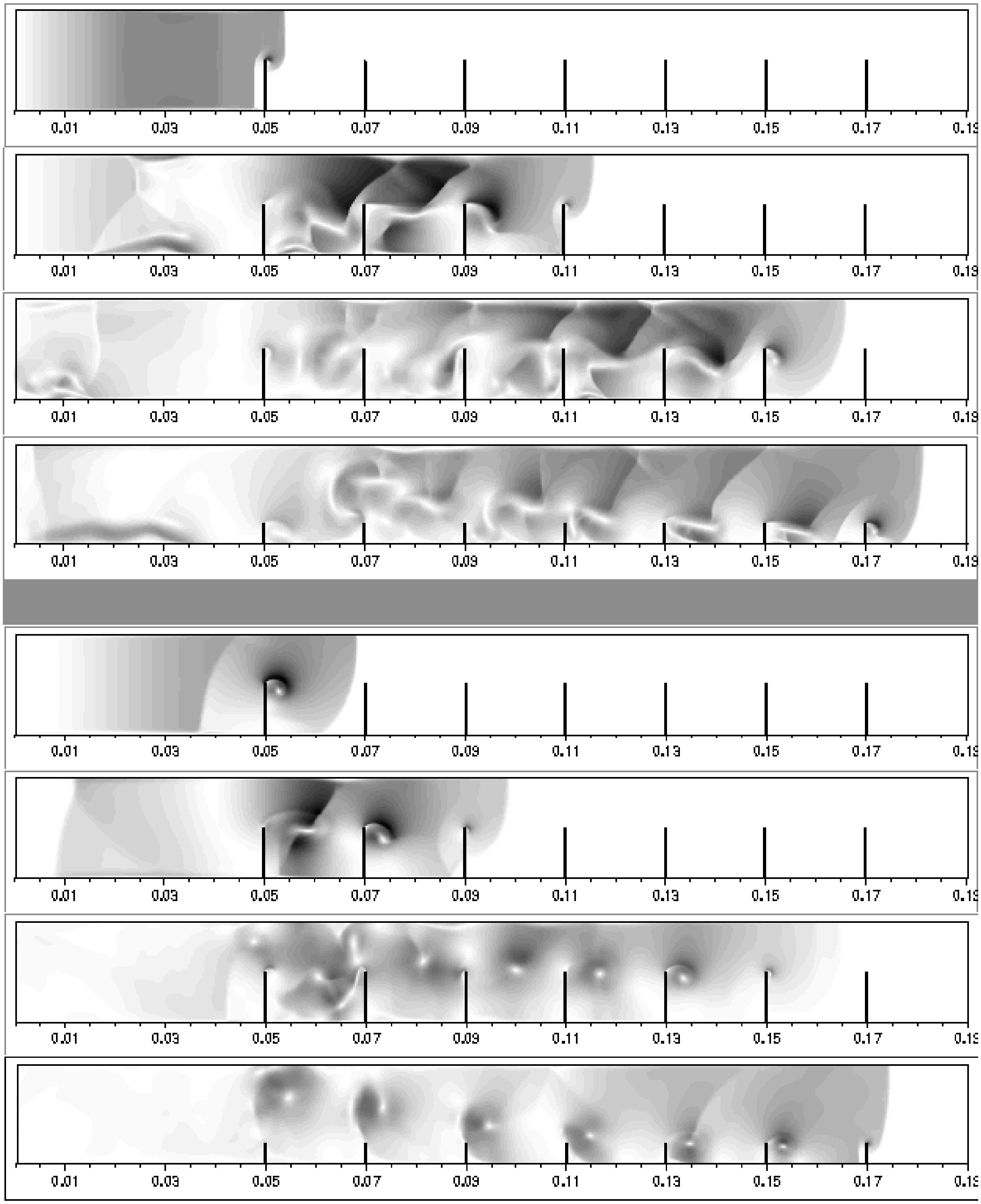

Figure 4: Mach Number Contours; from Top to Bottom: M_s=2 R=2 (t≈0.18τ, t≈0.54τ, t≈0.91τ), M_s=2 R=5 (t≈0.91τ), M_s=1.4 R=2 (t≈0.3τ, t≈0.5τ, t≈1.0τ), M_s=1.4 R=5 (t≈1.0τ).